

# Simulation of an inhomogeneous Fermi gas through the BCS-BEC crossover

R. Jáuregui, R. Paredes, L. Rosales-Zárate, and G. Toledo Sánchez

*Departamento de Física Teórica, Instituto de Física,  
Universidad Nacional Autónoma de México, A.P. 20-364, México 01000 D.F. México*

(Dated: February 20, 2019)

We perform a variational quantum Monte Carlo simulation of the transition from a Bose-Einstein condensate (BEC) to a Bardeen-Cooper-Schrieffer superfluid (BCS) at zero temperature. The model Hamiltonian involves an attractive short range two body interaction and the atoms number  $2N = 330$  is chosen so that, in the non-interacting limit, the ground state function corresponds to a closed shell configuration. The system is then characterized by the  $s$ -wave scattering length  $a$  of the two-particle collisions in the gas, which is varied from negative to positive values, and the Fermi wave number  $k_F$ . Based on an exhaustive analysis of the two-body problem, one parameter variational many-body wave functions are proposed to describe the ground state of the interacting Fermi gas from BCS to BEC states. We exploit properties of antisymmetrized many-body functions to develop efficient techniques that permit variational calculations for a large number of particles. It is shown that a virial relation between the energy per particle and the trapping energy is approximately valid for  $-0.1 < 1/k_F a < 1.4$ . The influence of the harmonic trap and the interaction potential as exhibited in two-body correlation functions is also analyzed.

## I. INTRODUCTION

The experimental realization of a degenerate Fermi gas in 1999<sup>1</sup>, boosted theoretical and experimental efforts to study interacting Fermi gases, in particular, the formation of molecules and highly correlated pairs from a balanced mixture of neutral interacting Fermi atoms in two different hyperfine spin states<sup>2,3,4,5,6,7,8</sup>. The possibility of tuning the strength of the interactions between particles in different spin states via Feshbach resonances, gives as a result the formation of Cooper pairs (molecules) for negative (positive) values of the scattering length  $a$ . At low temperatures, these pairs and molecules can form a Bardeen-Cooper-Schrieffer (BCS) superfluid state and a Bose-Einstein condensate (BEC) respectively. When crossing from the BCS to the BEC region, and viceversa,  $a$  grows in magnitude until it diverges at the resonance. In this limit the scattering length is no longer a relevant scale, and the properties of the gas become independent of the specific details of the interaction potential. This is the so called unitarity limit in which the gas is assumed to be universal, because its properties depend locally just on the density and the temperature, i.e., the only relevant scales in this universal quantum gas are the interparticle spacing and the Fermi energy. Consequently the gas properties can be expressed in terms of them and universal parameters<sup>3,7,8</sup>.

Previous treatments of the BEC-BCS crossover in degenerate atomic gases have been done using different approaches, we can mention the self-consistent many-body approach<sup>7</sup>, the effective field theory<sup>9</sup>, and more recently Quantum Monte Carlo calculations<sup>10,11,12,13,14</sup>. This last treatment has been mostly based on the fixed node Quantum Monte Carlo technique; in general, the two-component Fermi gas is considered as an homogeneous system although, experimentally, the fermionic atoms have an intrinsic inhomogeneous nature provided usually by a magnetic and/or optical trap. Such confining can be described by a harmonic potential. An interesting parameter calculated in those approaches is  $\beta$ , which relates the Fermi energy of the ideal Fermi gas  $E_{IFG}$  and the total energy of the interacting gas  $E$ . This is expected to acquire a universal value at unitarity. The predicted values for  $\beta$  ranges from -0.75 to -0.33<sup>7,9,10,12,13</sup>. First experimental estimates gave  $\beta \sim -0.36$ <sup>5</sup> and  $\beta \sim -0.49 \pm 0.04$ <sup>15</sup> while more recently values around  $-0.54$ <sup>16,17</sup> have been reported. The later results are based on measurements of the gas cloud radii at unitarity.

In a recent work<sup>18</sup>, we employed variational quantum Monte Carlo techniques (VQMC) to describe a balanced two-component interacting gas confined in a three-dimensional harmonic potential. There, we reported for the first time *direct* tests of the universality hypothesis in the unitarity limit including: (i) the verification of virial relations for  $N = 4, 10, 20, 35, 56, 84, 120$  and  $165$ , (ii) the variational estimate  $\beta_{fit} \geq -0.50_{(-0.04)}^{(+0.02)}$  using a linear fit of the energy per particle. In that paper we also briefly reported an analysis on observables like the system energy and density profiles in the BEC-BCS crossover. In particular we found  $N$ -independent energy curve features through the crossover.

In the present article we extend the analysis of<sup>18</sup>, paying special attention in exhibiting additional properties of the trial many body wave functions based on an extensive discussion of the two-body problem in the trap. Analytical compact expressions for two-body functions that contain collision and trapping effects are given. Particular properties of antisymmetrized many-body functions, let us develop efficient techniques here described that permit variational calculations for unusual large number of particles. The optimized wave functions allow the study of the influence of the harmonic trap and the interaction potential in energies, densities and two-body correlation functions all along the

crossover. The correlations between atoms in the same hyperfine state show the Pauli-blocking evolution as a function of  $a$ . Similarly, the correlations for atoms in different hyperfine state give information on formation of molecules and Cooper pairs. Here we report results for  $N = 165$  particles per each hyperfine state.

This work is organized as follows: in section II, we review the two body problem in order to construct the variational many-body wave functions for each region of the crossover. In section III we address the many-body system and exploit the structure of the variational wave functions to optimize numerical calculations. There, we describe in detail the procedure for the variational quantum Monte Carlo simulation and energy evaluation. Section IV contains the results for optimal variational parameters and energies, as well as densities and two-body correlation profiles. Our conclusions are presented in section V.

## II. THE TWO-BODY PROBLEM

Before studying the many-body problem we concentrate on the two-particle system. In the limit of low energies, it is expected that the scattering process represented by the  $s$ -wave scattering length  $a$ , determines the general features of the state of two colliding particles, regardless the detailed form of the interaction potential among them. For positive (negative) values of  $a$  the particles experience an *effective* repulsive (attractive) contact interaction that gives rise to a weakly bound (virtual) state. Strong modifications of  $a$  can be the result of either, small variations in the scattering potential or a tunable scattering energy for a given potential.

In dilute ultracold gases the Feshbach resonances enables the continuous variation of the scattering length. The appearance of a Feshbach resonance, in which a continuum or a molecular state can be formed, is a consequence of having two different channels for the binary collision, namely the open and closed channels, and the resonance occurs when the energies coincide with each other. In experiments where the resonances are broad, they can be approximated by a single-channel model. Near the crossover, the divergence of the scattering length poses difficulties in the interpretation of the  $s$ -wave contact interaction. Renormalization procedures have been designed<sup>19</sup> to allow the assignment of a *finite effective* scattering length which, through a regularized contact interaction, reproduces the observed behavior for specific collisions between atoms trapped by an external field.

The scope of this work is different. Here we consider a finite range attractive interaction that, for a given potential strength, yields scattering lengths through standard single-channel dispersion theory. Without using any explicit renormalization procedure, the behavior of two (and later many) trapped atoms is studied for short range interaction potentials as the strength is varied to cover scattering lengths  $-\infty < a < \infty$ . More precisely, we study the eigenstates of two particles of mass  $m$  trapped in a harmonic potential of frequency  $\omega$  and interacting through an isotropic attractive potential of finite range  $b/2$  given by

$$V(\vec{r}_{ij}) = V_0 e^{-2|\vec{r}_i^\uparrow - \vec{r}_j^\downarrow|/b}, \quad V_0 = -|V_0| \quad (1)$$

where the  $\uparrow$  and  $\downarrow$  superindices denote two different hyperfine atomic states and  $b \ll \sqrt{\hbar/m\omega}$ . The potential is chosen so that, in otherwise free space, it would admit a finite number of bound states as its strength is varied. We shall compare the results for trapped and unconfined particles, and analyze the role of the scattering length defined for a binary collision in free space. We shall also make a comparison with the regularized contact interaction results where  $a$  is directly introduced in the effective interaction. Even more important, the results of this section let us choose a two-body correlated basis which will be used in the many-body quantum Monte Carlo simulations.

The Schrödinger equation

$$\left[\frac{\hat{\mathbf{p}}^2}{2m} + V\right]\phi = E\phi \quad (2)$$

has analytical  $s$ -wave solutions<sup>20</sup>  $\phi(r) = v(r)/r$  both in the continuum

$$v(y) = c_1 J_{ib\sqrt{Em}/\hbar}(y) + c_2 J_{-ib\sqrt{Em}/\hbar}(y) \quad (3)$$

and in the bound states region

$$v(y) = c_+ J_{b\sqrt{|E|m}/\hbar}(y). \quad (4)$$

Here  $y = (b\sqrt{|V_0|m}/\hbar)e^{-r/b}$  and  $J_\nu$  represents the Bessel function of the first kind of order  $\nu$ . By imposing the proper boundary conditions and considering the limit  $E \rightarrow 0^+$ , the following expression is found for the  $s$ -wave scattering length

$$a = -b \left[ \frac{\pi}{2} \frac{N_0(b\sqrt{|V_0|m}/\hbar)}{J_0(b\sqrt{|V_0|m}/\hbar)} - \log(b\sqrt{|V_0|m}/2\hbar) - C \right] \quad (5)$$

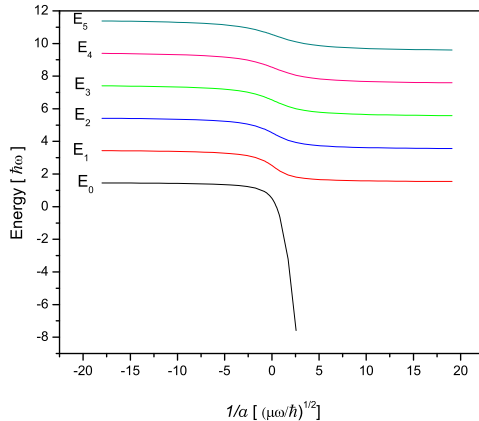


FIG. 1: Figure 1. Lowest  $s$ -wave relative energy eigenvalues for trapped two particles, Eq. (7).

with  $N_0$  the Bessel function of the second kind and order zero, and  $C$  the Euler constant. This scattering length diverges whenever  $J_0(b\sqrt{|V_0|m/\hbar}) = 0$ . If  $z_t, t = 0, 1, 2, \dots$  are the zeros of this Bessel function in increasing order, the potential  $V(r)$  admits just  $t$ -bound states for  $z_t < b\sqrt{|V_0|m/\hbar} < z_{t+1}$ . The discrete eigenvalues are determined by the boundary condition at  $r = 0$ ,  $J_{b\sqrt{|E|m/\hbar}}(b\sqrt{|V_0|m/\hbar}) = 0$ .

When the two-body collision process takes place in the presence of a harmonic potential that for simplicity we consider isotropic, the two-body Schrödinger equation can again be separated in a center of mass equation

$$\left[ \frac{\hat{\mathbf{P}}^2}{2M} + \frac{1}{2}M\omega^2\mathbf{R}^2 \right] \Phi(\mathbf{R}) = E_{CM}\Phi(\mathbf{R}), \quad (6)$$

and a relative coordinate equation

$$\left[ \frac{\hat{\mathbf{p}}^2}{2\mu} + \frac{1}{2}\mu\omega^2\mathbf{r}^2 + V(r) \right] \varphi(\mathbf{r}) = E\varphi(\mathbf{r}). \quad (7)$$

The former is the well known isotropic harmonic oscillator equation, and the latter can be numerically solved for a given range  $b/2$  and strength  $V_0$  of the potential.

The  $s$ -wave lowest eigenvalues  $E_n$  of Eq. (7) are illustrated in Fig. 1. While for

$$|V_0| < (z_0/b)^2\hbar\omega = \tilde{v}_0$$

the homogeneous two-body system has no bound states, Eq. (2), the trapped system has ground state energies that are near  $3/2\hbar\omega$  for small  $V_0$ . At  $V_0 \simeq \tilde{v}_0$  the scattering length diverges and, for such  $V_0$ , the confined system ground state has an energy eigenvalue near  $1/2\hbar\omega$  while the  $s$ -wave excited states have energies  $\sim (2n + 1/2)\hbar\omega$ . As  $V_0$  increases towards the  $a \rightarrow 0^+$  region the difference between the ground state energy for the trapped and homogeneous problem tends to zero. Besides, the first excited state energy approaches  $3/2\hbar\omega$ . In that limit the contact interaction in free space would admit a bound state with divergent binding energy. Here the finite value of  $V_0$  avoids this unphysical feature. If the field strength is further increased towards the second zero-energy resonance condition

$$|V_0| \rightarrow (z_1/b)^2\hbar\omega = \tilde{v}_1$$

the *first* excited state energy approaches the  $1/2\hbar\omega$  eigenvalue. The other excited states are separated by a  $\sim 2\hbar\omega$  factor. For even larger  $V_0$ , we observe that the difference between the *first* excited state energy for trapped and unconfined atoms also tends to zero.

All these numerical results are compatible with the regularized contact interaction analytical results<sup>21</sup> and confirm  $a$  as the relevant parameter for determining the general features of the interaction. That is,  $a$  determines the eigenvalues  $E > 1/2\hbar\omega$  irrespective to the number of states with  $E < 1/2\hbar\omega$ ; the states with  $E > 1/2\hbar\omega$  inherit the free space “scattering” states role, and the state with  $E = 1/2\hbar\omega$  replaces the zero-energy resonance at  $a \rightarrow \infty$ .

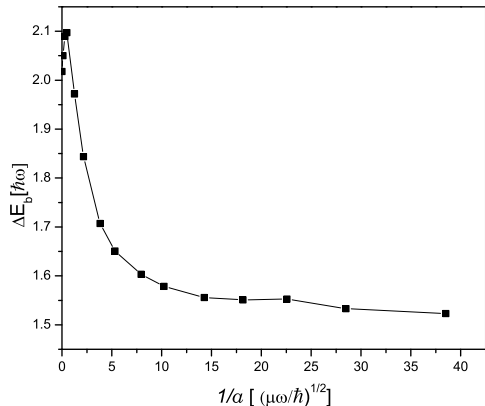


FIG. 2: Difference between the binding energies measured with and without harmonic trapping as a function of the inverse of the scattering length.

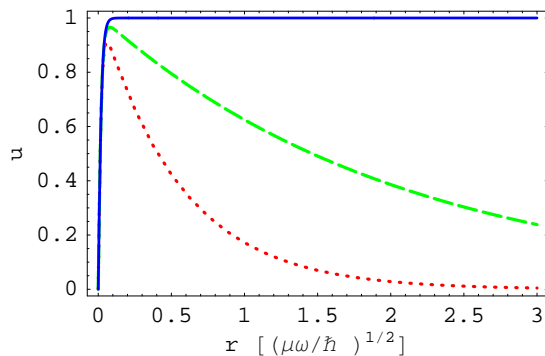


FIG. 3: Radial function  $u_a(r)$  for interacting particles in otherwise free space. The zero-energy resonant function  $u_\infty(r)$  (solid line) tends to a nonzero constant as  $r \rightarrow \infty$ , meanwhile  $u_{2.1}(r)$  (dashed line) and  $u_{0.58}(r)$  (dotted line) correspond to increasingly bound states.

For  $a > 1$ , the binding energy of the highest bound state associated to the homogeneous problem Eq. (2) is similar to the energy obtained by the contact interaction:  $\hbar^2/ma^2$ . But it is very different to the energy of the corresponding state in the trapped problem. Notice that in the confined two-body system the concept of binding energy must be revisited. For particles in free space, it is defined as the energy necessary to reach the continuum. For trapped atoms it could be defined as the difference between the energy eigenvalue of the state under consideration and the lowest eigenvalue  $E > \hbar\omega/2$ . The scenario behind measuring such energies would be the dissociation of the molecule keeping the trapping potential on. In Fig. 2, the difference between the binding energies measured with and without harmonic trapping, as a function of the inverse of the scattering length, is illustrated.

The general behavior of the  $u_a$   $s$ -ground state eigenfunctions ( $\varphi_a(r) = u_a(r)/r$ ) is illustrated in Fig. 3 for unconfined particles and Fig. 4 for trapped particles. In the latter case and for potential amplitudes lower than required for the first zero-resonance condition,  $|V_0| < (z_0/b)^2\hbar\omega$ , the structure of the ground state wave function deviates significantly from the free-space analog not just at long distances both also near the origin. We have found that, in this region, an analytical compact approximation to the numerical solution is given by

$$\varphi(r) \sim J_0(z_0 e^{-r/b}) e^{-m\omega r^2/4\hbar} (1 + c e^{-2r/b}) P(r/b)/r \quad (8)$$

with  $c$  independent of  $r$  and  $P(r/b)$  a polynomial of fourth order. An accuracy of this approximation higher than 0.01% has been achieved by the proper choice of  $c$  and  $P(r/b)$  both of which depend on  $V_0$  and  $b$ . For  $|V_0| \ll (z_0/b)^2\hbar\omega$ , the polynomial  $P(r/b)$  is almost linear while for  $|V_0| \leq (z_0/b)^2\hbar\omega$ , it results that  $c \approx 0$ .

For  $|V_0| \geq (z_0/b)^2\hbar\omega$ , and in the region of positive  $a$ , the *ansatz* for the ground state function

$$\varphi(r) = v(y(r)) e^{-m\omega r^2/4\hbar} g(r)/r \quad (9)$$

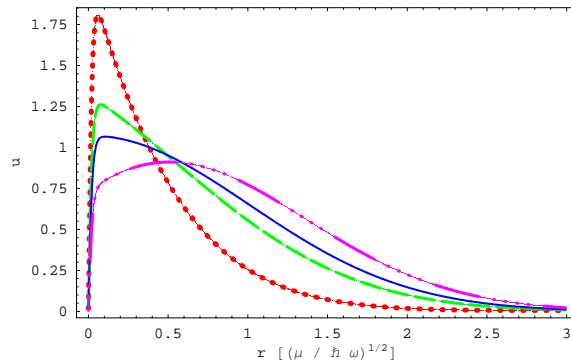


FIG. 4: Radial function  $u_a(r)$  for interacting particles in the presence of the trapping potential. The dot-dashed curve corresponds to the ground  $s$ -state for a negative scattering length  $u_{-0.6}(r)$ , the zero-energy resonant function  $u_\infty(r)$  is given by the solid curve, while  $u_{2.1}(r)$  by the dashed one and  $u_{0.58}(r)$  by the dotted line. In this figure the wave functions have been properly normalized.

with  $v$  defined in Eq. (4) is numerically accurate to a 1% level. These analytical approximations to the exact solutions of the two-body problem will be exploited in the study of the many-body system.

The structure of Eq. (9) for the eigenfunctions at  $|a| \rightarrow \infty$  let us understand the origin of the eigenvalue  $\sim 1/2\hbar\omega$ . In this case,  $v(y(r))$  takes care of the boundary condition  $v(0) = 0$  so that the effective equation for  $\varphi(r) \cdot (r/v)$  is almost identical to that of the one dimensional harmonic oscillator without the requirement of becoming null at  $r = 0$ , thus admitting the possibility  $E \sim 1/2\hbar\omega$ .

Summarizing, the main results which are relevant in the forthcoming treatment of the ultra cold many-body system are:

- i) The  $s$ -wave scattering length as given by Eq. (5) still determines the general features of the interaction at low energies.
- ii) The zero energy resonance of the inhomogeneous problem, is shifted down with respect to the homogeneous one so that for  $|a| \rightarrow \infty$  the  $s$ -wave states have energies  $\sim (2n + 1/2)\hbar\omega$  ( $n=0,1,2,\dots$ ) instead of  $(2n + 3/2)\hbar\omega$ , as effect of the interaction.
- iii) For parameters of the potential with  $-\infty < a < \infty$  around the first zero-energy resonance condition, analytical approximations to the exact solutions of the ground state two body trapped problem are given by Eqs. (8-9).

### III. THE MANY-BODY SYSTEM

Let us consider the system made up of  $2N$  fermions in two, equally populated, hyperfine states ( $N = N_\uparrow = N_\downarrow$ ) confined in an isotropic three-dimensional harmonic trap of frequency  $\omega$ . The system is allowed to interact via binary collisions between particles of different hyperfine states. The Fermi gas is considered to be at zero temperature and the two-body collision process is approximated by the single-channel model described in the previous section, Eq. (1). The Hamiltonian describing such a system is:

$$H = \sum_{i,j=1}^N -\frac{\hbar^2}{2m} (p_i^2 + p_j^2) + \frac{1}{2}m\omega (r_i^2 + r_j^2) + \sum_{i,j} V_{ij}. \quad (10)$$

where  $m$ ,  $\vec{r}_i$  and  $\vec{p}_i$ , are the mass, position and momentum of each fermion respectively.

#### A. Variational Monte-Carlo simulations

In a variational calculation, for a given form of the interaction potential, the optimal value of any variational parameter  $\lambda$  in the wave function  $\Psi_\lambda$ , is determined by imposing that the expectation value of the Hamiltonian, Eq. (10) in our problem, to be a minimum with respect to such parameter. So that,

$$\frac{\partial E(\lambda)}{\partial \lambda} = 0 \quad \text{where} \quad E(\lambda) = \frac{\langle \Psi_\lambda | H | \Psi_\lambda \rangle}{\langle \Psi_\lambda | \Psi_\lambda \rangle}. \quad (11)$$

For a system of  $N$  atoms, computing the expectation value requires the evaluation of a  $3N$ -dimensional integral. The main idea of the Monte Carlo method is not to evaluate the integrand at every one of the quadrature points, but rather at only a relatively small representative sampling  $M$ , where the sequence of configurations are distributed according to  $|\Psi_\lambda|^2$ <sup>29</sup>. We use Metropolis algorithm<sup>30</sup> which ensures that the desired probability distribution is approached asymptotically.

In this article, the generic form of the variational wave function will be different according to the region of the BEC-BCS crossover. Accordingly, explicit details will be given for each region separately.

### 1. Variational calculation for weakly interacting fermions

First, let us consider the region in the potential parameters space where, for a given range  $b/2$ , the amplitude of the potential is so small that no bound states are allowed in the homogeneous two-body problem. There, it is expected that the trapped ideal Fermi gas configuration gives a rough description of the system. Accordingly, a Jastrow-Slater wave function of the form

$$\Psi_\lambda^{JS} = \Phi_{IFG} \cdot F_\lambda^J \quad (12)$$

is assumed. Here  $\lambda$  is a variational parameter,  $\Phi_{IFG}$  is the Fermi gas wave function given by the product of Slater determinants (one for each hyperfine state) describing a noninteracting system of harmonically trapped atoms, and the Jastrow function  $F_\lambda^J$  will explicitly include the effects of the interaction potential.

The inputs of the Slater determinants are the single-particle eigenstates of a non-interacting particle in a harmonic trap,  $\phi_{\mathbf{n}}(\mathbf{x})$ , with quantum numbers  $\mathbf{n}$  at the position  $\mathbf{x}$ . This construction ensures that the wave function is totally antisymmetric under the exchange of identical atoms. The energy of each single particle state is characterized by three integer quantum numbers  $\mathbf{n} \equiv (n_x, n_y, n_z)$ :

$$E_{\mathbf{n}} = \hbar\omega \left( \frac{3}{2} + n_x + n_y + n_z \right), \quad (n_i = 0, 1, 2, \dots) \quad (13)$$

being  $(n+1)(n+2)/2$ -degenerated. A typical basis state has the form:

$$\phi_{n_x, n_y, n_z}(\mathbf{x}) = \left( \frac{1}{a_{ho}^2 \pi} \right)^{3/4} \prod_{\xi=x,y,z} \frac{H_{n_\xi}(\xi/a_{ho})}{\sqrt{2^{n_\xi} n_\xi!}} e^{-\xi^2/2a_{ho}^2} \quad (14)$$

where  $H_{n_\xi}(\xi/a_{ho})$  are the Hermite functions of order  $n_\xi$  and  $a_{ho} = \sqrt{\hbar/m\omega}$ . In this paper, we consider closed shell configurations so that the ground state is built up by taking all single-particle states with energies increasing from  $E_0 = 3\hbar\omega/2$  up to the Fermi energy  $E_F = (\mathcal{M}_F + 3/2)\hbar\omega$ , where  $\mathcal{M}_F$  is the maximum energy level for a given number of particles. For large  $N$ ,  $E_F \sim (6N)^{1/3}\hbar\omega$ , whose corresponding radius is  $R_F^2 = 2E_F/m\omega^2$ .

In the literature of interacting bosons and fermions, the Jastrow wave function usually takes the form of a product  $\prod_{i,j} f_{ij}$  of correlation functions  $f$  that depend on the degrees of freedom of the pair  $i, j$  of interacting particles. In Refs.<sup>10,22,23,24</sup>  $f$  is a function of the interparticle distance  $r$  that solves the free-space interacting two-body problem up to a healing distance  $d$  after which it is restricted to become constant. In those works, the parameter  $d$  is chosen by minimizing the energy.

In this paper, we shall consider trial many-body wave functions which yield a continuous  $F_\lambda^J$  and continuous derivatives; the optimal variational parameter  $\lambda$  of the trial wave function for the many body system will establish an effective  $d$  as we illustrate below. In fact, we have studied two options for the Jastrow function:

(i)  $f_{ij} = \exp(-\lambda V_0 e^{-2r_{ij}/b})$ , so that,

$$F_\lambda^J = \exp[-\lambda \sum_{i_\uparrow, j_\downarrow} V(|\vec{r}_{i_\uparrow} - \vec{r}_{j_\downarrow}|)] \quad (15)$$

$$(ii) \quad f_{ij} = J_0(z_0 e^{-r/\lambda})(1 + c e^{-2r/\lambda})P(r/\lambda)/r \quad (16)$$

The first choice of the variational wave function (15) have the advantage of becoming exact when no interactions between hyperfine states are allowed ( $\lambda = 0$ ) which is the trapped ideal Fermi gas limit where the only correlations are those imposed by the Pauli exclusion principle. It is inspired on previous calculations for the nuclear matter<sup>25,26</sup>,

where an appropriate choice of the potential allows to explore dynamically the interplay of the nuclear-to-quark matter regime. In addition, this form of the variational wave function allows to estimate the energy expectation value by computing only spatial dependent functions in a Monte Carlo simulation<sup>27</sup>, as we show below.

The second choice is inspired on the general structure of the two-body wave functions in free space at low energies. It allows to numerically explore shorter potential ranges than the first option (15). It implicitly reproduces the fact, first noticed in BCS theories, that even the slightest interaction can lead to two-body long-range-correlations implicit in the polynomial  $P(r/b)$ . Besides, it should reproduce effects of the trap for the short interparticle separations through the factor proportional to  $c$ . Deviations from  $\lambda = b$  should be interpreted as a many-body effect.

The structure of the variational wave function for the BCS region, allows to simplify the expectation value of the kinetic-energy operator through an integration by parts<sup>25</sup>. That is,

$$\langle \Psi_\lambda | \sum_{i=1}^N \frac{\mathbf{p}_i^2}{2m} + \frac{1}{2} m \omega r_i^2 | \Psi_\lambda \rangle = E_{IFG} + 2\lambda^2 \langle W \rangle_\lambda . \quad (17)$$

where  $E_{IFG}$  is the energy of the non-interacting trapped Fermi gas. For a closed shell configuration (all single particle states with energies below  $E_F = (\mathcal{M}_F + 3/2)\hbar\omega$  are occupied) and a small number of atoms, this energy can be computed using the following equation<sup>28</sup>

$$\frac{E_{IFG}}{N\hbar\omega} = \frac{3}{4}\mathcal{M}_F + \frac{3}{2}, \quad (18)$$

instead of the large  $N$  limit,  $E_{IFG} = 3NE_F/4$ , which produces a slightly underestimated value. Eq. (18) is valid in general.

The extra term  $W$  in Eq. (17), reflects the increase in the kinetic energy of the system, relative to the Fermi-gas estimate, due to interactions. In the case of Eq. (15) it is given by

$$W = \sum_k^{3N} \frac{1}{2m} [\partial_k V(\vec{r}_{i\uparrow}, \vec{r}_{j\downarrow})]^2 \quad (19)$$

where the derivative is over all three-spatial components of the atoms in the system. Finally, we set the form of the expectation value of the total energy as:

$$E(\lambda) = E_{IFG} + 2\lambda^2 \langle W \rangle_\lambda + \langle V \rangle_\lambda . \quad (20)$$

The two functions that remain to be evaluated ( $V$  and  $W$ ) are local; their expectation values may be computed via Monte Carlo techniques as described above. A similar approach can be used in the case corresponding to the Jastrow function Eq. (16).

We have performed calculations of the energy for a fixed value of  $N$ , the range  $b/2$  and the scattering length  $a$ , exploring for several values of the variational parameter  $\lambda$ , picking up the one which minimizes the energy. Each run used about  $10^3$  steps for thermalization and about  $10^4$  more to take data. In the first rows of Table I, we report the numerical optimal energies using the first choice for the Jastrow function and a potential range  $b/2 = 0.015\sqrt{\hbar/m\omega}$ . Similar results are obtained when the second choice of  $F^J$  is used. The data corresponds to  $N = 165$ , which fills eight shells ( $\mathcal{M}_F = 8$ ) for the harmonic potential in three dimensions;  $k_F$  represents the Fermi wave number associated to the ideal Fermi gas energy  $E_{IFG} = (\hbar k_F)^2/2m$ . For such number of particles the corresponding energy per particle for an ideal Fermi gas is  $E_{IFG}/2N = 7.5\hbar\omega$ . The quoted error bars take into account the minimization process itself as well as effects of the initial conditions that could be not erased during the thermalization process. It is important to point out that the variational energy for the highest  $1/k_F a$  value coincides with that obtained from a perturbative calculation using a contact interaction as can be verified from expressions obtained in Ref.<sup>28</sup>. As  $a$  approaches the crossover region it is expected that the trial function Eq.(12) will not describe properly the interatomic correlations since pairing effects become essential so that the quantum numbers in the Slater determinants in  $\Phi_{IFG}$  are not representative of the physical situation.

The optimal value of  $\lambda$  determines the shape of the Jastrow correlation function. As an illustration, in Fig. 5 we plot the behavior of the two particle  $f_{ij}^\lambda$  function of Eq. (15) for  $b = 0.03\sqrt{\hbar/m\omega}$  and two different values of the scattering length  $1/k_F a = -0.3873$  and  $-15.8888$  respectively. We observe that the distance at which  $f_{ij}^\lambda \sim 1$  is larger than the potential range, this suggests long distance correlated pairs, as expected for a BCS-like pairs. This result is also in good agreement previous findings reported in<sup>10,23</sup> where the healing distance is used as a variational parameter.

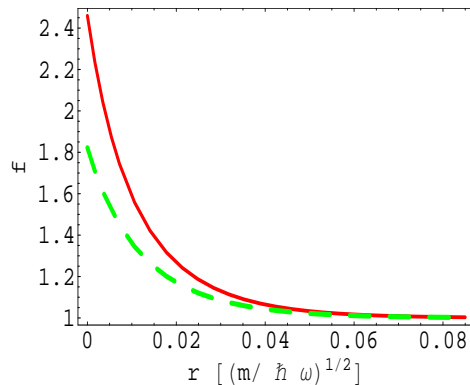


FIG. 5: First choice Jastrow correlation function for  $b = 0.03\sqrt{\hbar/m\omega}$ , dashed and solid lines correspond to  $1/k_F a = -0.3873$  and  $-15.8888$  respectively.

## 2. Variational calculation on the BCS-BEC crossover region

In a theory originally put forth by Eagles<sup>34</sup> and later by Leggett<sup>35</sup>, it was proposed that a BCS wave function of the form

$$\Psi_\lambda = \mathcal{A} [\phi(1_\uparrow, 1_\downarrow)\phi(2_\uparrow, 2_\downarrow)\dots\phi(N_\uparrow, N_\downarrow)], \quad (21)$$

with  $\mathcal{A}$  the antisymmetrizer operator that ensures the correct properties under particle exchanges, was more generally applicable than just to the weakly interacting limit<sup>34</sup>: a BCS-like wave function could eventually describe the ground state from a Cooper pairing region to BEC of composite bosons made up of two fermions.

Following this point of view, here we propose the family of single-parameter variational wave functions for the BCS-BEC crossover regime, taking  $\phi(i_\uparrow, j_\downarrow)$  as a variational extrapolation of the ground state solution of the trapped two body problem

$$\phi(\vec{r}_{i_\uparrow}, \vec{r}_{j_\downarrow}) \cong \varphi(r_{ij})e^{-\lambda|\vec{r}_{i_\uparrow} + \vec{r}_{j_\downarrow}|^2/4}, \quad (22)$$

The variational parameter  $\lambda$  modulates the optimal shape of the cloud. The wave function (21) guarantees that the Monte Carlo dynamics will be guided by effects of both paired-particles relative  $\vec{r}_{ij} = \vec{r}_i - \vec{r}_j$  and center of mass  $\vec{R}_{ij} = (\vec{r}_i + \vec{r}_j)/2$  vectors.

It is worth to mention that at difference with previous calculations<sup>10,12</sup> here, by explicitly including the inhomogeneous features of the density, we are able to explore the *trapped* atoms as a whole as they evolve into the interacting regime. Besides, at difference with the mean field approach, no optimal individual particle wave functions are searched, but the global effect of the interaction on the paired-particles wave function.

To estimate the energy in the BEC side, the algorithm described for the BCS region is not useful because it depends on the explicit structure of the wave function, written in a Jastrow-Salter form. In order to set the variational energy in a form suitable for Monte Carlo estimations we exploit the two-body structure of the potential and the primitive wave functions  $\phi$ . The antisymmetrized wave function (21) can be explicitly written as

$$\Psi_\lambda = \sum_{\mathcal{P}} (-1)^{\mathcal{P}} \prod_{i=1}^N \phi(i, \mathcal{P}(i)) \quad (23)$$

where the summation is taken over all possible permutations  $\mathcal{P}$  on set  $\downarrow$ , and  $\phi(i, \mathcal{P}(i))$  are wave functions having the form of Eq. (22) and argument  $(\vec{r}_{i_\uparrow}, \vec{r}_{\mathcal{P}(i)_\downarrow})$ . We can split the Hamiltonian of the system in a pair-like sum, using the center of mass and relative coordinates of possible pairs as:

$$\begin{aligned} H = & \sum_i^N \left[ \frac{\mathcal{P}_{i, \mathcal{P}_0(i)}^2}{2\mu} + \frac{\mu}{2} \omega^2 r_{i, \mathcal{P}_0(i)}^2 \right. \\ & \left. + V_{i, \mathcal{P}_0(i)}(r) + \frac{P_{i, \mathcal{P}_0(i)}^2}{2M} + \frac{M}{2} \omega^2 R_{i, \mathcal{P}_0(i)}^2 \right] \end{aligned}$$



$$+ \sum_{i,j \neq \mathcal{P}_0(i)} V(r_{i,j}) \quad (24)$$

with  $\mathcal{P}_0$  any given permutation.

Eq. (22) let us write:

$$\begin{aligned} H\Psi_\lambda &= \left[ N\epsilon_0 + N\frac{3\hbar\omega\lambda}{2} \right] \Psi_\lambda \\ &+ (1 - \lambda^2) \sum_{i, \mathcal{P}} (-1)^{\mathcal{P}} \frac{M}{2} \omega^2 R_{i, \mathcal{P}(i)}^2 \prod_{l=1}^N \phi(l, \mathcal{P}(l)) \\ &+ \sum_{\mathcal{P}} (-1)^{\mathcal{P}} \sum_{i,j \neq \mathcal{P}(i)} V(r_{i,j}) \prod_{l=1}^N \phi(l, \mathcal{P}(l)) \end{aligned} \quad (25)$$

with  $\epsilon_0$  the ground state eigenvalue of the two body-problem. To evaluate the last two terms via a Monte Carlo simulation we proceed to complete the potential by adding and subtracting the term used in the two-body solution, then:

$$\begin{aligned} H\Psi_\lambda &= \left[ N\epsilon_0 + N\frac{3\hbar\omega\lambda}{2} + \sum_{i,j} V(r_{i,j}) \right] \Psi_\lambda \\ &+ \sum_{i, \mathcal{P}} (-1)^{\mathcal{P}} \prod_{l \neq i} \phi(l, \mathcal{P}(l)) \cdot \left[ (1 - \lambda^2) \frac{M}{2} \omega^2 R_{i, \mathcal{P}(i)}^2 \right. \\ &\left. - V(r_{i, \mathcal{P}(i)}) \right] \phi(i, \mathcal{P}(i)) \end{aligned} \quad (26)$$

which can also be written in terms of the minors  $C_{i\alpha}(\Psi_\lambda)$  associated to the  $\Psi_\lambda$ :

$$\Psi_\lambda = \sum_{\alpha=1}^N C_{i\alpha}(\Psi_\lambda) \phi_{i,\alpha} \quad (27)$$

where  $\phi_{i,\alpha}$  represents any of the  $i$ -row wave functions.

$$\begin{aligned} H\Psi_\lambda &= \left[ N\epsilon_0 + N\frac{3\hbar\omega\lambda}{2} + \sum_{i,j} V(r_{i,j}) \right] \Psi_\lambda \\ &+ \sum_{i,\alpha} C_{i,\alpha} \cdot \left[ (1 - \lambda^2) \frac{M}{2} \omega^2 R_{i,\alpha}^2 - V(r_{i,\alpha}) \right] \phi(i, \alpha) \end{aligned}$$

This expression results quite convenient for the simulations to be performed, where one can also take advantage from the relation between minors and the elements of the inverse of the transposed matrix<sup>27</sup>,

$$\bar{\phi}_{i,\alpha} \equiv (\phi^T)_{i\alpha}^{-1} = \frac{C_{\alpha,i}(\Psi_\lambda^T)}{\Psi_\lambda^T} = \frac{C_{i,\alpha}(\Psi_\lambda)}{\Psi_\lambda}. \quad (28)$$

Thus, we can write

$$\begin{aligned} H\Psi_\lambda &= \left[ N\epsilon_0 + N\frac{3\hbar\omega\lambda}{2} + \sum_{i,j} V(r_{i,j}) \right. \\ &\left. + \sum_{i,\alpha} \phi_{i,\alpha} \bar{\phi}_{i,\alpha} \left[ (1 - \lambda^2) \frac{M}{2} \omega^2 R_{i,\alpha}^2 - V(r_{i,\alpha}) \right] \right] \Psi_\lambda \end{aligned} \quad (29)$$

As in the BCS calculation, we can sample the system using a Metropolis-Monte Carlo algorithm and estimate the energy as a function of the variational parameter.

$1/k_F a$	$V_0 \lambda_{opt}$ $\pm 0.05$	$E/2N$ [ $\hbar\omega$ ]	$\epsilon_0$ [ $\hbar\omega$ ]	$\langle m\omega^2 R^2 \rangle$ [ $\hbar\omega$ ]
-15.88895	-0.6	7.450 $\pm$ 0.004	1.49	9.0 $\pm$ 0.2
-9.60883	-0.6	7.425 $\pm$ 0.005	1.48	9.0 $\pm$ 0.2
-4.26632	-0.6	7.374 $\pm$ 0.009	1.46	9.03 $\pm$ 0.2
-2.02479	-0.9	7.345 $\pm$ 0.012	1.42	9.03 $\pm$ 0.2
-0.3873	-0.9	7.217 $\pm$ 0.052	1.23	9.03 $\pm$ 0.2
$1/k_F a$	$\lambda_{opt}$ $\pm 0.005$	$E/2N$ [ $\hbar\omega$ ]	$\epsilon_0$ [ $\hbar\omega$ ]	$\langle m\omega^2 R^2 \rangle$ [ $\hbar\omega$ ]
-0.43893	0.142	7.07 $\pm$ 0.06	1.15	8.67 $\pm$ 0.2
-0.22418	0.134	6.65 $\pm$ 0.06	0.99	7.57 $\pm$ 0.2
-0.10071	0.160	6.37 $\pm$ 0.06	0.79	6.58 $\pm$ 0.2
-0.03745	0.182	6.10 $\pm$ 0.06	0.72	5.64 $\pm$ 0.2
0	0.186	5.25 $\pm$ 0.08	0.50	5.32 $\pm$ 0.2
$1/k_F a$	$\lambda_{opt}$ $\pm 0.005$	$(E/2N) - \epsilon_0/2$ [ $\hbar\omega$ ]	$\epsilon_0$ [ $\hbar\omega$ ]	$\langle m\omega^2 R^2 \rangle$ [ $\hbar\omega$ ]
0.13959	0.190	4.78 $\pm$ 0.07	0.39	4.92 $\pm$ 0.2
0.34876	0.191	4.18 $\pm$ 0.07	2.45	4.50 $\pm$ 0.2
0.69684	0.256	3.57 $\pm$ 0.07	9.95	3.75 $\pm$ 0.2
1.04427	0.270	3.35 $\pm$ 0.06	22.65	3.51 $\pm$ 0.2
1.39107	0.380	3.14 $\pm$ 0.08	40.76	2.99 $\pm$ 0.2
2.08293	0.665	2.60 $\pm$ 0.08	93.96	2.95 $\pm$ 0.2
2.77266	0.90	2.0 $\pm$ 0.1	171.157	2.89 $\pm$ 0.2
3.46055	0.94	1.38 $\pm$ 0.15	274.99	2.59 $\pm$ 0.25
4.1469	0.99	1.1 $\pm$ 0.15	404.64	2.59 $\pm$ 0.25
5.51634	0.99	0.95 $\pm$ 0.15	756.643	2.59 $\pm$ 0.40
7.38482	1.0	0.82 $\pm$ 0.2	3746.22	2.39 $\pm$ 0.40

TABLE I: Optimal variational parameter  $\lambda$ , energy per particle, two-body ground  $\epsilon_0$  energies and mean value of the trap potential energy per particle  $\langle m\omega^2 R^2 \rangle$  all of them calculated as a function of  $1/k_F a$  considering  $2N = 330$  particles.

In Table I, we illustrate the results obtained for several scattering lengths when the range of the potential is  $b/2 = 0.00375\sqrt{\hbar/m\omega}$  before the unitarity limit,  $1/k_F a = 0$ , and  $b/2 = 0.0025\sqrt{\hbar/m\omega}$  for  $k_F a \geq 0$ . Actually, calculations were performed for several potential ranges  $b/2$  all over the crossover. The  $b/2$  ranges reported in this table are the shortest for which reliable numerical results were obtained. In that sense they can be regarded as a  $b \rightarrow 0$  numerical limit. Table I includes the optimal variational parameter  $\lambda$  and the corresponding energy per particle  $E/2N$ . For  $1/k_F a < -0.45$  the variational energy  $E/2N$  for the wave-function (21-22) is higher than that obtained with the Jastrow-Slater trial wave-function, while for  $1/k_F a > -0.45$  the situation is inverted and the *BCS*-wave function gives a lower upper bound for  $E/2N$ . A similar effect has been found in Ref.<sup>12</sup> for the homogeneous gas. Beyond the unitarity region, *i. e.* for  $a > 0$ , the contribution  $\epsilon_0/2$  coming from the trapped ground state two-body eigenvalue has been subtracted. As mentioned before,  $|\epsilon_0|$  does not necessarily coincide with the binding energy for the trapped molecule. For  $1/k_F a > 4$  an optimal value of  $\lambda \sim 1$  yielding a local minima was found. Nevertheless, for  $\lambda > 1$  the corresponding mean value of the energy can be made arbitrarily small by considering  $\lambda$  large enough. This variational instability is expected at the extreme BEC region for any attractive potential of finite range as discussed previously in Ref.<sup>11</sup> for a homogeneous gas. It could eventually be avoided by adding a repulsive interaction at distances much smaller than the range  $b/2$  as suggested in the original work by Leggett<sup>35</sup>. Implementing this idea within our numerical approach is very difficult since already  $b \ll \sqrt{\hbar/m\omega}$ .

In Table I, we also report the mean value of the potential energy per particle associated to the trap  $\langle m\omega^2 R^2 \rangle$ . This value is more feasible of experimental verification and does not require of any assumption concerning the role played by the internal molecular energy  $\epsilon_0$ . Notice that in the crossover region with  $-0.1 < 1/k_F a < 1.4$ ,  $E/2N - \epsilon_0/2 \sim \langle m\omega^2 R^2 \rangle$ .

The relevance of the numerical results reported here becomes more evident when it is taken into account that the energy as a function of the scattering length exhibits a universal behavior as shown in Ref.<sup>18</sup>.

### 3. Unitarity

At unitarity,  $|a| \rightarrow \infty$ , we have estimated the energy using a variational wave function of the form Eq. (23). The numerical results were presented and broadly discussed in Ref.<sup>18</sup> in connection with the universality hypothesis. Here

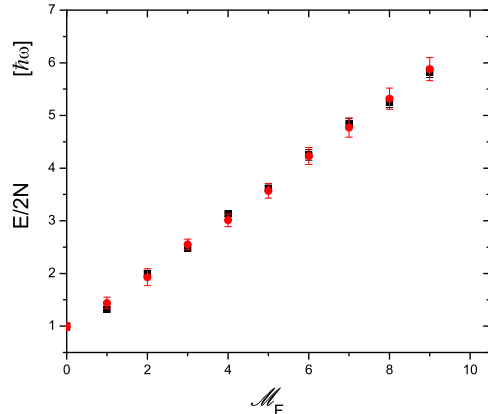


FIG. 6:  $s$ -ground state variational energy and  $\langle m\omega^2 R^2 \rangle$  for trapped particles at unitarity as a function of the Fermi number  $\mathcal{M}_F$  for closed shells.

we want to emphasize that the numerical errors at unitarity are larger than those obtained for the closest scattering lengths as shown in Table I. The reason can be traced back to the qualitative difference between the two-body wave function  $u_{ij}$  defined by Eq. (9). The high delocalization of the unitarity paired-atoms-wave function makes more difficult the evaluation of the energy expectation value at this limit.

As reported in Ref.<sup>18</sup>, we have obtained  $\beta = -0.50^{(+0.02)}_{(-0.04)}$  as an upper bound to the universal parameter defined by  $E = E_{IFG}\sqrt{1+\beta}$  for a trapped degenerate gas by making a fit to the straight line that results from evaluating the ground state energy for the closed shell configurations corresponding to  $N = 4, 10, 20, 35, 56, 84, 120, 165$  and 220 particles as a function of the shell number  $\mathcal{M}_F$ :

$$E_U/2N\hbar\omega \sim 0.53 \pm 0.01(\mathcal{M}_F + 1.95 \pm 0.06) \quad (30)$$

In Fig. 6, we show  $E(\mathcal{M}_F)$  together with the mean value  $\langle m\omega^2 R^2(\mathcal{M}_F) \rangle$ .

## B. Densities and correlations

In addition to the energy per particle several properties of the ground state have been calculated as a function of the scattering length; in particular, we investigated the single-particle and the two-particle correlation functions. In the following we illustrate these correlation functions for  $N = 165$  for the optimized wave function in each regime; the BCS ( $a < 0$ ), the unitarity ( $a \rightarrow \infty$ ) and the molecular ( $a > 0$ ) regimes. We have chosen examples in the crossover with  $|1/k_F a| < 1$  due to its expected independence on the details of the calculation.

The single-particle correlation function, that is, the density profile as a function of the distance to the center of the harmonic trap has already been illustrated in Fig. 2 of Ref.<sup>18</sup>. There, we can see that the trap effect is reflected by decreasing the particle density until vanishing around the Fermi radius i.e., the inhomogeneous environment created by the harmonic confinement affects all the regimes as it is already evident for an ideal Fermi gas in the Thomas-Fermi approximation<sup>33</sup>. The shape of the BCS density profile is similar to the one corresponding to the ideal gas but with a different mean radius. The density increases at the center while decreases as it goes to the edge of the trap. This deviations can be attributed to the optimal value of the variational parameter which captures the interaction and correlation effects in the many-body system. This kind of shape prevails up to the unitarity limit. The major differences in the particle density for each regime occur around the center of the trap, particularly for the BEC regime. For this regime most of the paired atoms are located near the origin.

In Figure 7 we plot the two-particle correlation function  $g_{\uparrow\uparrow}$  for particles in the same hyperfine state. It was computed by finding the fraction of atoms in the same hyperfine state within a relative distance  $(r, r + dr)$  irrespective of the center of mass position as generated by the Monte Carlo sampling. The result was divided by  $N(N-1)/2$  to account for the combinatorial of the atoms. The Jastrow-Slater wave function in the limit of an ideal Fermi gas ( $\lambda = 0$ ), exhibits the Pauli blocking arising from the fermionic nature of the atoms (triangle symbols). The BCS trial wave function shows an slightly diminished Pauli blocking for short distances (square symbols). In the molecular side

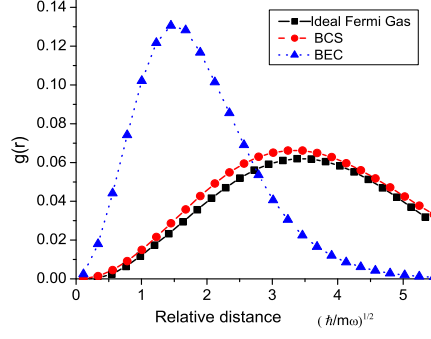


FIG. 7: Correlation function  $G(r)$  for particles in the same hyperfine state as a function of their relative distance. Square, circle, and triangle symbols correspond to the ideal Fermi gas, BCS ( $1/k_F a = -0.224$ ), BEC ( $1/k_F a = 0.697$ )

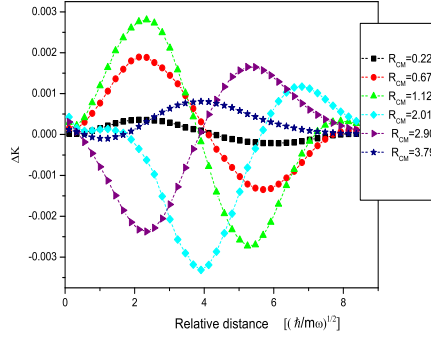


FIG. 8: Probability difference  $\Delta K(r_{ij}, R_{cm})$  that two particles with antiparallel spin are found separated a distance  $r_{ij}$  in the BCS and ideal regimes. Each curve in this figure correspond to different spherical radii  $R_{cm}$  measured from the center of the trap. Calculations are performed at  $1/k_F a = -0.224$ .

it is observed that particles in the same hyperfine state can be found around the same region (triangle symbols). Although at the deep BEC regime Pauli blocking still inhibit the presence of atoms in the same hyperfine state, the radius at which it is evident becomes very short. As a consequence, if an exclusively attractive interacting potential is considered and it is large enough, Pauli blocking is not able to avoid a variational collapse for  $1/k_F a > 7.5$ . All of these correlations decreases for long relative distances as a consequence of the presence of the trap.

In Figure 3 of Ref.<sup>18</sup> we compared the results for the two-particle correlation functions of atoms in different hyperfine states in the BEC regime with respect to the ideal regime, as a function of the relative distance  $r_{ij} = |r_{i\uparrow} - r_{j\downarrow}|$  among them. It was evaluated in a similar way to that corresponding to  $g_{\uparrow\uparrow}$  taking care of the proper normalization factor ( $N^2$ ) and keeping the information of the center of mass position of the pairs. Molecule formation was indicated by the increase in the correlation for very short distances,  $r_{ij} \ll \sqrt{\hbar/m\omega}$ . Most molecules are formed for  $R_{cm} < 1.09\sqrt{\hbar/m\omega}$ . An enhancement of the probability of finding pairs of particles separated at relative distances of the order of  $r \sim \sqrt{\hbar/m\omega}$  indicated molecular condensation effects.

Figure 8 illustrates the differences between the two-particle correlation functions of atoms in different hyperfine states,  $\Delta K(r_{ij}, R_{cm})$  for the ideal and BCS regimes. As in Fig. 3 of Ref.<sup>18</sup>, it shows results for a set of radius  $R_{cm}$  measured from the center of the trap. We observe that, although not zero, the difference is very small (see the abscissae scale) compared to the result for the BEC regime, in addition strong oscillations in  $r_{ij}$  are seen for all the  $R_{cm}$ .

#### IV. CONCLUSIONS

We have studied an interacting two-component Fermi gas confined in an isotropic harmonic potential in three dimensions. In particular, we investigated the transition from a Bose-Einstein condensate (BEC) to a Bardeen-Cooper-Schrieffer state (BCS) at zero temperature for a system composed of  $N = 165$  particles of equal mass in each spin-state. This transition was followed as a function of the scattering length  $a$ .

The interaction between particles was considered to be an attractive potential with very short range interaction ( $b \rightarrow 0$ ). Analytical compact expressions for two-body functions that contain collision and trapping effects were obtained. It is expected that for such short range interactions the many-body ground state depends just on the product of the scattering length and the Fermi wave number  $k_F a$ . In fact, when the number of particles is chosen so that closed shell configurations would arise in the ideal trapped gas limit, a normalized curve can be assigned to the ground state energy as a function of  $1/k_F a$  which is independent of Fermi shell number  $\mathcal{M}_F$ <sup>18</sup>.

To model the gas, we proposed many-body wave functions for the BCS superfluid ( $a < 0$ ) and the BEC ( $a > 0$ ) sides. For small negative values of  $a$  we described the atomic gas by a Jastrow-Slater wave function. While, for other values of  $a$ , following Eagles<sup>34</sup> and Leggett<sup>35</sup> proposal, a wave function written as the antisymmetric product of two-particle states was used. Using variational Quantum Monte Carlo simulations we determined the properties of the many body system for the ground state as a function  $a$ . For a given interaction range, we determined the single variational parameter  $\lambda_{opt}$  that minimizes the energy per particle of the whole system. By considering several values of the range of the potential and studying the stability of the results, the limit  $b \rightarrow 0$  was numerically approached. The optimal variational wave functions lead to predictions for the main properties of the trapped system like energies, mean radii, one and two-point correlation functions.

The extreme BEC region was not analyzed due to the instability which arises when no repulsive potential of range shorter than  $b/2$  is introduced. In our calculations the extreme BEC region starts when the variational parameter  $\lambda$  yields the minimum energy for  $\lambda_{opt} > 1$ . For  $\lambda_{opt} = 1$  the two-particle wave function for each pair of fermions corresponds to ideal molecules in the ground trapped state. For  $\lambda_{opt} > 1$  the effect of Pauli blocking is supersede by the very strong short range attractive potential.

The starting point of the crossover from the BCS side could be regarded as the value of  $1/k_F a$  for which the antisymmetric product of two-particle states gives a lower expectation value of the energy with respect to the Jastrow-Slater wave function. According to our calculations this already occurs at  $1/k_F a \sim -0.45$ . This value is similar to that at which a variational calculation based on scaled antisymmetric product of harmonic oscillator wave functions can not be applied since no minima exists<sup>28</sup>.

The system energy was computed all along the crossover, and at unitarity the  $\beta$  was determined to be  $\beta_{fit} = -0.50_{+0.04}^{-0.02}$ . We should emphasize that our calculations indicate that the universal hypothesis yields results consistent with theoretical calculations even for a small  $N$ . In addition it was shown that not only at unitarity but also over the crossover region  $-0.45 < 1/k_F a < 2$  the mean value of the atomic gas squared radius can be used to give a rough estimate of the energy per particle, since  $\langle m\omega^2 r^2 \rangle \sim E/2N - \bar{\epsilon}_0/2$ , where  $\bar{\epsilon}_0$  is the two-body ground state energy  $\epsilon_0$  for trapped fermions for  $a > 0$  and zero for  $a \leq 0$ . In the BEC side  $\epsilon_0$  is almost identical to the binding molecule energy up to the region close to unitarity.

We calculated the one-particle and the two-particle correlation functions for the BCS and BEC regimes and for the unitary limit. The results show that the correlation length between pairs can be much larger than the interaction potential range. As expected, the inhomogeneous environment resulting from the harmonic confinement affects all the regimes. We observe that in the BCS regime, the paired atoms have a large correlation length particularly for  $0.6 < R_{cm} < 1.2\sqrt{\hbar/m\omega}$ . Pauli blocking effects were also sensible to trapping and interaction strength. Thus, we conclude that the approximate analytical wave function used to describe the trapped interacting gas gives a good compact representation of the system through the crossover region.

**Acknowledgments** This work was partially supported by Conacyt México, under grant 41048-A1 and DGAPA-UNAM contract PAPIIT IN117406-2.

---

<sup>1</sup> B. DeMarco and D. S. Jin, Science **285**, 1703 (1999).

<sup>2</sup> S. Jochim, M. Bartenstein, A. Altmeyer, G. Hendl, S. Riedl, C. Chin, J. H. Denschlag, and R. Grimm, Science **302**, 2101 (2003); M. Greiner, C. A. Regal, and D. S. Jin, Nature **426**, 537 (2003); M. W. Zwierlein, C. A. Stan, C. H. Schunck, S. M. F. Raupach, S. Gupta, Z. Hadzibabic, and W. Ketterle, Phys. Rev. Lett. **91**, 250401 (2003); K. E. Strecker, G. B. Partridge, and R. G. Hulet, Phys. Rev. Lett. **91**, 080406 (2003).

<sup>3</sup> K. M. O'Hara, S. L. Hemmer, M. E. Gehm, S. R. Granade, J. E. Thomas, Science **298**, 2179(2002); M. E. Gehm, S. L. Hemmer, S. R. Granade, K. M. O'Hara, and J. E. Thomas, Phys. Rev. A **68**, 011401(R) (2003).

- <sup>4</sup> M. Bartenstein, A. Altmeyer, S. Riedl, S. Jochim, C. Chin, J. H. Denschlag, and R. Grimm, Phys. Rev. Lett. **92**, 120401 (2004).
- <sup>5</sup> T. Bourdel, J. Cubizolles, L. Khaykovich, K. M. F. Magalhaes, S. J. M. F. Kokkelmans, G. V. Shlyapnikov, and C. Salomon, Phys. Rev. Lett. **91**, 020402 (2003).
- <sup>6</sup> T. Bourdel, L. Khaykovich, J. Cubizolles, J. Zhang, F. Chevy, M. Teichmann, L. Tarruell, S.J.M.F. Kokkelmans, and C. Salomon **93**, 050401 (2004).
- <sup>7</sup> H. Heiselberg, Phys. Rev. A **63**, 043606 (2001).
- <sup>8</sup> T.-L. Ho, Phys. Rev. Lett. **92**, 090402 (2004).
- <sup>9</sup> W. Vincent Liu, Phys. Rev. Lett. **96**, 080401 (2006).
- <sup>10</sup> J. Carlson, S. Y. Chang, V. R. Pandharipande, and K. E. Schmidt, Phys. Rev. Lett. **91**, 050401 (2003).
- <sup>11</sup> S. Y. Chang, V. R. Pandharipande, J. Carlson, and K. E. Schmidt, Phys. Rev. A **70**, 043602 (2004).
- <sup>12</sup> G. E. Astrakharchik, J. Boronat, J. Casulleras, and S. Giorgini, Phys. Rev. Lett. **93**, 200404 (2004).
- <sup>13</sup> D. Lee, Phys. Rev. B **73**, 115112 (2006).
- <sup>14</sup> D. Blume, J. von Stecher, C. H. Greene, Phys. Rev. Lett. **99**, 233201 (2007).
- <sup>15</sup> J. Kinast, A. Turlapov, J. E. Thomas, Q. J. Chen, J. Stajic, and K. Levin, Science **307**, 1296 (2005).
- <sup>16</sup> G. B. Partridge, W. Li, R. I. Kamar, Y. an Liao, and R. G. Hulet, Science **311**, 503 (2005).
- <sup>17</sup> J. T. Stewart, J. P. Gaebler, C. A. Regal, and D. S. Jin, arXiv:cond-mat/0607776 v1(2006)
- <sup>18</sup> R. Jáuregui, R. Paredes and G. Toledo Sánchez, Phys. Rev. A **76**, 011604(R)(2007).
- <sup>19</sup> E. L. Bolda, E. Tiesinga, and P. S. Julienne, Phys. Rev. A **66**, 013403 (2002)
- <sup>20</sup> W. Rarita and R. D. Present, Phys. Rev. **51**, 788 (1937).
- <sup>21</sup> T. Busch, B.G. Englert, K. Rzażewski, and M. Wilkens, Foundations of Phys. **28**, 549 (1998).
- <sup>22</sup> D. Schiff and L. Verlet, Phys. Rev. **160**, 208 (1967).
- <sup>23</sup> V. R. Pandharipande and H. A. Bethe, Phys. Rev. C **7**, 1312 (1973).
- <sup>24</sup> V. R. Pandharipande and K.E. Schmidt, Phys. Rev. A **15**, 2486 (1977).
- <sup>25</sup> C. J. Horowitz, E. J. Moniz and J. W. Negele, Phys. Rev. D **31**, 1689 (1985); C. J. Horowitz and J. Piekarewicz, Nucl. Phys. A **536**, 669 (1992).
- <sup>26</sup> G. Toledo Sánchez, and J. Piekarewicz, Phys. Rev. C **65**, 045208 (2002).
- <sup>27</sup> D. Ceperly, G.V. Chester and M.H. Kalos, Phys. Rev. B **16**, 3081 (1977).
- <sup>28</sup> R. Jáuregui, R. Paredes and G. Toledo Sánchez, Phys. Rev. A. **69** 013606 (2004).
- <sup>29</sup> Steven E. Koonin, *“Computational Physics”* (Benjamin Cummings, Menlo Park, 1986).
- <sup>30</sup> N. Metropolis, A. Rosenbluth, M. Rosenbluth, A. Teller, and E. Teller, J. Chem Phys. **21**, 1087 (1953).
- <sup>31</sup> J. E. Thomas, J. Kinast, and A. Turlapov, Phys. Rev. Lett. **95**, 120402 (2005).
- <sup>32</sup> G. A. Baker, Phys. Rev. C **60**, 054311 (1999).
- <sup>33</sup> D.A. Butts and D.S. Rokhsar, Phys. Rev. A **55**, 4346 (1997).
- <sup>34</sup> D. M. Eagles, Phys. Rev. **186**, 456 (1969).
- <sup>35</sup> A. J. Leggett, J. Phys. (Paris) **41**, C7 (1980).